Thermodynamics and Kinetics of the Adsorption of Carbon Monoxide on Supported Gold Catalysts Probed by Static Adsorption Microcalorimetry: The Role of the Support

Xinyu Xia,[†] Jennifer Strunk,[†] Wilma Busser,[†] Massimiliano Comotti,[‡] Ferdi Schüth,[‡] and Martin Muhler*,[†]

Laboratory of Industrial Chemistry, Ruhr-University Bochum, D-44780 Bochum, Germany, and Max-Planck-Institut für Kohlenforschung, D-45470 Mülheim an der Ruhr, Germany

Received: November 6, 2008; Revised Manuscript Received: April 3, 2009

The interaction of carbon monoxide and oxygen with gold particles supported on zinc oxide, alumina, and titania was investigated by microcalorimetry. Multiple processes were detected during CO adsorption, including adsorption of CO on the gold particles and support, oxidation of CO, and formation of carbonates. The rate of O_2 adsorption was much slower than that of CO adsorption. The heats and entropies of CO adsorption on the Au sites indicated that the interaction between CO and Au supported on TiO_2 is much stronger than that between CO and Au supported on ZnO. The Au/ZnO sample had the largest amount of lattice oxygen (7.6 μmol/g), which reacted with CO to give CO_2.

1. Introduction

The hydrogenation of carbon monoxide provides two essential products for the chemical industry. Over catalysts containing open d shell metals such as Fe, Co, Ni, or Ru, the main products are methane and higher hydrocarbons

$$CO + 3H_2 \rightleftharpoons CH_4 + H_2O \quad (1)$$

Over commercially applied $Cu/ZnO/Al_2O_3$ catalysts and over ZnO/Cr_2O_3 used in the old high-pressure process, methanol is the dominating product[1,2]

$$CO + 2H_2 \rightleftharpoons CH_3OH \quad (2)$$

In recent years, supported gold catalysts have been applied in both reactions 1and 2, providing new insight into the mechanism of methanol synthesis. Sakurai and Haruta[3,4] reported on the hydrogenation of CO_2, where in the temperature range from 200 to 400 °C, only CH_3OH was obtained over Au/ZnO, while methane was also formed and became dominant with increasing temperature over Au/TiO_2 and Au/Al_2O_3. Obviously, the effect of the support on the catalytic properties of the gold catalysts is rather strong. Over Cu/Al_2O_3 and Cu/TiO_2, the yield of methanol was found to be smaller compared to that of Cu/ZnO, but the formation of methane was not observed.[5] Zhao et al.[6] reported a shift in the product selectivity to higher alcohols, especially ethanol and 1-propanol, during CO hydrogenation at 573 K and 2.5 MPa over Au/ZnO compared to that of ZnO, and Mpela et al.[7] found a high selectivity to hydrocarbons, when incorporating Au in ZnO.

Even in case of the well-established ternary $Cu/ZnO/Al_2O_3$ catalyst, the role of ZnO is still a subject of controversy. ZnO is essential for the stabilization of copper particles and is effective against sulfur poisons; it also strongly interacts with Cu particles forming Cu−Zn sites and even a copper−zinc alloy under highly reducing conditions.[8−10] Whether these new species and ZnO because of its oxygen vacancies are also involved in the catalytic process is a controversial topic.[11−15] Recent studies applying adsorption calorimetry and CO as a probe molecule provided strong evidence for these strong metal−support interactions in Cu/ZnO catalysts.[16,17]

For the ternary Cu catalyst, CO_2 is considered the main carbon source of methanol[18] because isotope labeling (^{14}C) showed that methanol is formed directly from CO_2.[19−21] A transient kinetic study provided further evidence for this hypothesis.[22] It is difficult to distinguish between CO and CO_2 as the carbon source of methanol because the $Cu/ZnO/Al_2O_3$ catalyst is also highly active for the water−gas shift reaction[21,23−26]

$$CO + H_2O \rightleftharpoons CO_2 + H_2 \quad (3)$$

On ZnO, however, both pathways from CO and CO_2 as carbon sources have been suggested, and an oxygen vacancy has been assumed as the active site.[27−29] The reaction pathway starting from CO as a carbon source was suggested to be the energetically favorable one, and recent catalytic activity studies of oxygen-deficient ZnO revealed a beneficial influence of a higher degree of oxygen deficiency of ZnO on the catalytic activity in methanol synthesis from CO as a carbon source.[30]

For a deeper understanding of the mechanism of CO hydrogenation over Au catalysts, it is first necessary to investigate the interaction with CO. Volumetric measurements show that CO adsorbs only to a small extent on Au particles and that a larger fraction of the uptake occurs on the support.[31−34] CO adsorbed on Au sites at the interface of reducible supports such as ZnO and TiO_2 reacts with surface lattice oxygen atoms.[35−37] Because of this oxidation, the adsorption of CO on Au/TiO_2 is not fully reversible.[33]

The heats of adsorption of CO on pure Au and supported Au catalysts have been derived from temperature-programmed desorption (TPD) or from quantitatively applied spectroscopies,[38−45] showing that the heat of adsorption of CO on titania-supported Au (>70 kJ/mol) is larger than that on pure Au (<60 kJ/mol). Using the spectroscopic intensity of the CO band in a polarization modulation−infrared reflection absorption spectroscopy (PM-IRAS) study, Diemant et al.[46] found a size dependence of the CO adsorption energy on the Au particles, which had been deposited on a flat TiO_2 surface. While the initial

* To whom correspondence should be addressed. E-mail: muhler@techem.rub.de. Telephone: +49 234 32 28754. Fax: +49 234 32 14115.
[†] Ruhr-University Bochum.
[‡] Max-Planck-Institut für Kohlenforschung.

10.1021/jp809804v CCC: $40.75
Published on Web 05/01/2009

TABLE 1: Characteristics of the Used Au Catalysts

sample	Au (wt %)	BET area (m^2/g)	Au particle size d_c (nm)[b]	surface atomic concentration (%)[a]			
				O	C	cation	Au
Au/ZnO	1.0[c]	45	2.8 ± 1.1[c]	51.22	4.82	43.71 (Zn)	0.25
Au/Al_2O_3	1.0[c]	198	3.1 ± 1.3[c]	61.00	5.18	33.51 (Al)	0.31
Au/TiO_2 #1	1.0[c]	56	3.0 ± 1.3[c]	62.59	10.38	26.61 (Ti)	0.42
Au/TiO_2 #2	1.51[d]	56	3.8 ± 1.5[d]				

[a] Values are from X-ray photoelectron spectroscopy. Sensitivity factors are 0.66 for O 1s, 0.25 for C 1s, 0.185 for Al 2p, 1.8 for Ti 2p, 4.8 for Zn $2p_{3/2}$, and 4.95 for Au 4f. [b] Diameter of Au particles observed by TEM. [c] Ref 57. [d] Ref 58.

heat of adsorption of CO was 74 kJ/mol with Au particles with mean lateral diameters of 2 nm, a value of only 62 kJ/mol was obtained for Au particles with mean lateral diameters of 4 nm.[46] The stronger adsorption of CO on small Au particles was also found in a CO TPD study on Au deposited on well-ordered alumina and iron oxide films.[47] On Au/CeO_2, it was found spectroscopically that CO adsorbs more strongly on cationic gold sites when compared with metallic gold.[48] Generally, the binding of CO to cationic Au, Ag, and Cu sites was found to be stronger than that on the corresponding metals.[49] This was proposed as the origin of the higher light-off temperature of CO oxidation over Au/CeO_2 samples containing mainly cationic Au particles compared with those containing mainly metallic Au particles.[48] A comprehensive overview of CO adsorption on gold surfaces and different supported gold catalysts can be found in ref 50. Ref 51 presents recent advances in understanding of CO adsorption on Au using density functional theory (DFT).

Indirect methods for obtaining heats of adsorption of CO on Au catalysts such as TPD and different spectroscopic methods may be not fully reliable because CO may react with these catalysts. In TPD measurements, a certain amount of dosed CO can be oxidized and desorbs as CO_2 instead of CO, thus leading to an underestimation of the CO adsorption energy. The isotherms derived from the spectroscopic intensity of the adsorbed species also do not reflect this fraction of CO. Therefore, it is advantageous to measure the heats of adsorption of CO adsorption on Au catalysts directly using calorimetry. The only microcalorimetric study on Au catalysts found in the literature was performed by Tripathi and co-workers.[52,53] Because the support in their work was Fe_2O_3, which reacts strongly with CO, it was not possible to obtain the heats of adsorption of CO on Au/Fe_2O_3.

Oxygen is also a useful molecule to probe the surface properties of supported gold catalysts, which allows the detection of the presence of oxygen vacancies. Molecular oxygen essentially does not chemisorb on pure Au.[54] TPD measurements estimated that the amount of oxygen chemisorbed on Au/TiO_2 was about 0.45 μmol/g,[55] and the heat of adsorption of oxygen on Au catalysts has not been reported yet. In this contribution, we studied the adsorption of CO and O_2 on Au/ZnO, Au/Al_2O_3, and Au/TiO_2 by microcalorimetry. The adsorption thermodynamics and kinetics were derived, and on the basis of these results, the role of the support is discussed. The role of oxygen vacancies as active sites in the synthesis of methanol over Au/ZnO was investigated recently.[56]

2. Experimental Section

The Au/ZnO, Au/Al_2O_3, and Au/TiO_2 (labeled as Au/TiO_2 #1) samples with 1 wt % Au were prepared by colloidal deposition.[57] Another Au/TiO_2 sample (labeled as Au/TiO_2 #2) was supplied by the World Gold Council (labeled as Au/TiO_2 #02−4 in ref 58), which was prepared by deposition precipitation. Characterization results of these samples are summarized in Table 1.

Prior to the calorimetric measurements, an amount of 0.2−0.3 g of the sample was pretreated at 523 K in 10% O_2 in Ar (purity: O_2, 99.995%; Ar, 99.999%; flow rate of 25 Nml/min, Nml = normal milliliters; calibrated for $T = 273$ K and $p = 10^5$ Pa) at ambient pressure in a U-tube reactor for 4 h. The sample was preserved in a sealed glass capsule after cooling to room temperature under inert gas without exposure to air. The microcalorimeter setup and the measurement procedures were the same as reported in previous studies.[16,59] The adsorption temperature was $T = 303$ K. The volume of the adsorption cell was $V = 129 \pm 1$ cm^3, and it was calibrated in each measurement. In this setup, the heat flow was measured by a Tian-Calvet microcalorimeter, and the pressure was recorded every second through a pressure transducer. The uptake can then be derived from the pressure measurements. The purity of the adsorptive gases was 99.997% for CO and 99.995% for O_2.

After the sample capsule had been introduced into the sample cell, the whole setup was baked for 72 h at 418 K, then cooled to 303 K. The sample capsule was crushed with a linear motion feedthrough and evacuated for 30 min. Then, the first CO adsorption experiment was performed. The dosing procedure was carried out until the equilibrium pressure reached 800 Pa. Afterward, the setup with the sample was evacuated overnight at 303 K to investigate the reversibility of CO adsorption, and the second series of CO adsorption measurements, followed by evacuation, was performed. Then, adsorption measurements using O_2, followed by evacuation, and another series of adsorption experiments with O_2 were performed. After O_2 adsorption and evacuation, the Au/Al_2O_3 sample was probed with CO again, and the Au/ZnO sample was oxidized in the calorimeter cell at $T = 418$ K and $p_{O_2} = 100$ kPa for 12 h, before another series of CO adsorption experiments was carried out. In addition to the pretreatment in 10% O_2 in Ar, another sample of the Au/TiO_2 #2 catalyst was pretreated in flowing H_2 at 523 K in the U-tube reactor.

Because Au catalysts are very effective in the oxidation of CO by gaseous O_2, the influence of the O_2 leakage had to be considered with great care. After crushing of the sample capsule and before the first dose of CO in each adsorption measurement, N_2 was filled into the microcalorimeter setup, and it took about 50 min before the baseline of the calorimetric signal became stable. The amount of O_2 leaking into the cell is given by

$$\frac{r_{leak} t V}{RT} \times 21\%$$

where r_{leak} is the leakage rate (in Pa/s) derived from the increase in pressure under static vacuum conditions as a function of time, t is the time interval, V is the volume of the dosing section and the measurement cells, and 21% is the molar content of O_2 in air. Taking the experiment of CO adsorption on the Au/ZnO

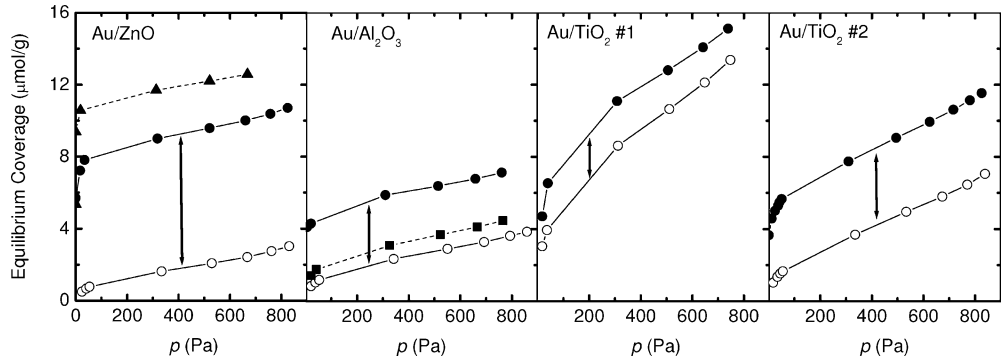

Figure 1. Isotherms of CO adsorption on the Au catalysts at 303 K as a function of the pretreatment. (●) First isotherm after the pretreatment at 523 K in flowing 10% O_2 in Ar. (○) Second isotherm after CO adsorption and evacuation at 303 K. (▲) After oxidation in 100 kPa O_2 at 418 K within the calorimeter and evacuation. (■) After the O_2 isotherm (adsorption at $p < 1$ kPa) at 303 K and evacuation. Vertical arrows indicate the difference in uptake between the first and second CO isotherm obtained after evacuation at 303 K as summarized in Table 2.

TABLE 2: Amount of Oxygen Species Reacting with CO Derived from Figure 1

	difference in amount of consumed CO between the first and second isotherm[a]	
sample	(μmol/g)	(μmol/g)
Au/ZnO	7.6	0.17
Au/Al_2O_3	3.6	0.019
Au/TiO_2 #1	2.3	0.04
Au/TiO_2 #2	4.4	0.08

[a] The first isotherm was obtained after the pretreatment at 523 K in flowing 10% O_2 in Ar and the second isotherm after CO adsorption and evacuation at 303 K.

sample (0.23 g) as an example, with $r_{leak} = 1.9 \times 10^4$ Pa/s, $t =$ 3200 s, $V = 129$ cm^3, and $T = 303$ K, we determine the amount of O_2 in the setup before CO adsorption as 0.013 μmol, which consumes 0.026 μmol CO at most. For the first adsorption measurement of this sample, the CO uptake in the first dose was 5.7 μmol/g or 1.31 μmol for the whole sample mass; for the first dose of the repeated measurement, the CO uptake was 0.49 μmol/g or 0.11 μmol. Thus, the influence of O_2 due to the very low leak rate before adsorption is negligible. Similar results were also obtained for the measurements with the other samples.

3. Results

3.1. CO Uptake. Figure 1 shows the CO adsorption isotherms obtained after different pretreatments. On each freshly oxidized sample pretreated at 523 K in flowing 10% O_2 in Ar, the uptake reached over 4 μmol/g at a very small pressure, with p^{eq} being under the detection limitation; afterward, it increased linearly with pressure. In the measurements repeated after evacuation, the uptake at small pressure was considerably smaller, and the isotherms were clearly irreversible. The Au/ZnO sample had the largest difference between the specified uptake in the freshly oxidized state and in the CO-reduced state amounting to 7.6 μmol/g (Table 2). The uptakes of the two Au/TiO_2 samples differ strongly, which may result from the different preparation methods influencing the surface properties.

The CO isotherms shown in Figure 1 also point to an effect of the O_2 dosing conditions during the pretreatment of the uptake of CO. For the Au/ZnO sample, after it had been oxidized with 100 kPa O_2 in the adsorption cell at 418 K for 12 h, the uptake of CO was higher than after the sample had been oxidized with flowing 10% O_2 in Ar in the ex situ pretreatment at 523 K for 4 h. For the Au/Al_2O_3 sample, we observed that after measurement of the O_2 isotherm at 303 K at a static pressure of less than 10 Pa and evacuation, the uptake of CO was much smaller than after the ex situ pretreatment with flowing 10% O_2 in Ar.

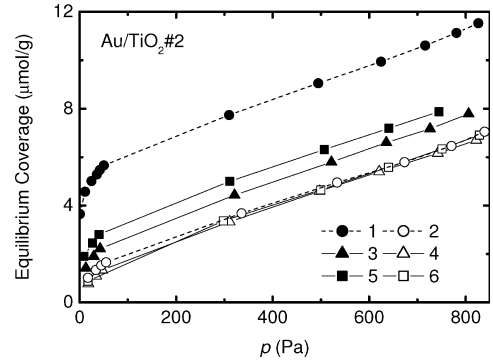

Figure 2. Isotherms of CO adsorption on sample Au/TiO_2 #2 at 303 K as a function of the pretreatment. First (1, ●) and second (2, ○) adsorption after the pretreatment at 523 K in flowing 10% O_2 in Ar. First (3, ▲) and second (4, △) adsorption after the pretreatment in flowing H_2 at 523 K. First (5, ■) and second (6, □) adsorption after the O_2 isotherm (adsorption at $p < 1$ kPa) at 303 K and evacuation.

Figure 2 presents the isotherms of CO adsorption on sample Au/TiO_2 #2 after different pretreatments. No matter how the sample was pretreated, after the first measurement of the CO adsorption isotherm followed by evacuation, the second isotherm of each of the following series of CO adsorption experiments is similar.

Figure 3 shows the adsorption kinetics of the first dose of CO on the four Au catalysts. For the Au/ZnO sample, it took several hundred seconds to reach adsorption equilibrium, and the kinetics can be evaluated by the following equation[60]

$$n = n^{eq}[1 - (1 + k_a ct)\exp(-k_a ct)] \quad (4)$$

where n is the coverage as a function of time, n^{eq} is the equilibrium coverage, k_a is the rate constant of adsorption in (Pa^{-1} s^{-1}), and c is the ratio between the decrease of pressure and the increase of fractional coverage in Pa. The obtained k_a values were all in the range from 10^{-5} to 10^{-6} Pa^{-1} s^{-1}. For the Au/Al_2O_3 and Au/TiO_2 samples, when $t > 100$ s, the coverage versus time traces deviated from eq 4. The adsorption rate became considerably slower than expected from the adsorption kinetics (eq 4), indicating there is a slower overlapping process that retards adsorption.

Figure 4 presents the differential heats of adsorption (q^{diff}) of CO on the oxidized samples, which also demonstrates that the processes occurring during the adsorption of CO are not reversible. High values of q^{diff} were observed at low coverage of the first of each pair of measurements; the exposure of Au/ZnO to CO had the highest value of over 336 kJ/mol for the sample oxidized inside the calorimetric vessel at 418 K.

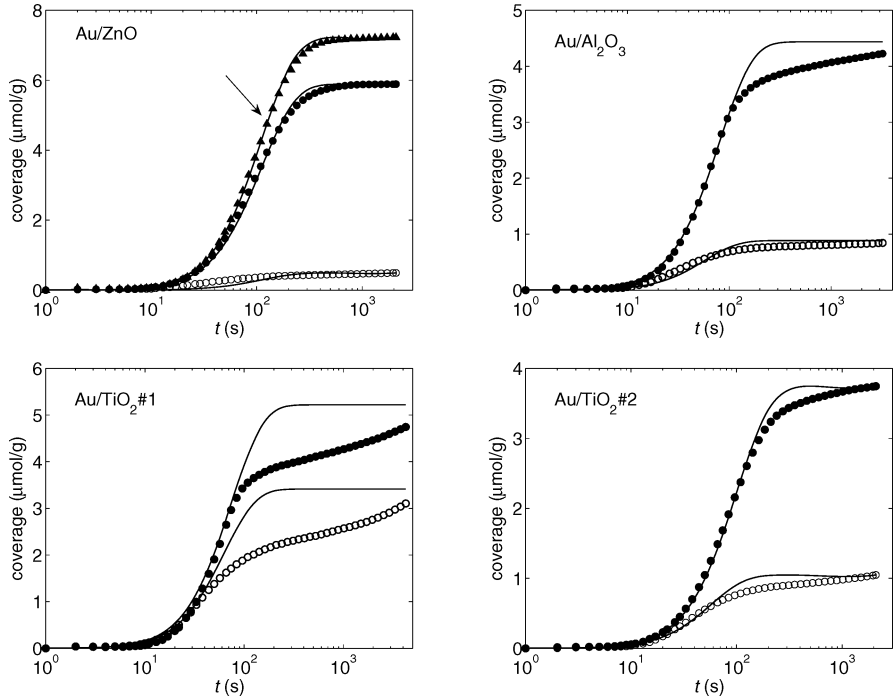

Figure 3. Adsorption kinetics of CO on the Au catalysts. Circles are experimental data; solid lines are theoretical values from eq 5. (●) First CO dosing experiment directly after the pretreatment at 523 K in flowing 10% O_2 in Ar. (○) First CO dosing experiment of the second series of CO adsorption measurements subsequent to evacuation. For Au/ZnO, the first CO dosing experiment is shown, upper left (▲) marked by an arrow, subsequent to oxidation in 100 kPa O_2 at 418 K within the calorimeter and evacuation.

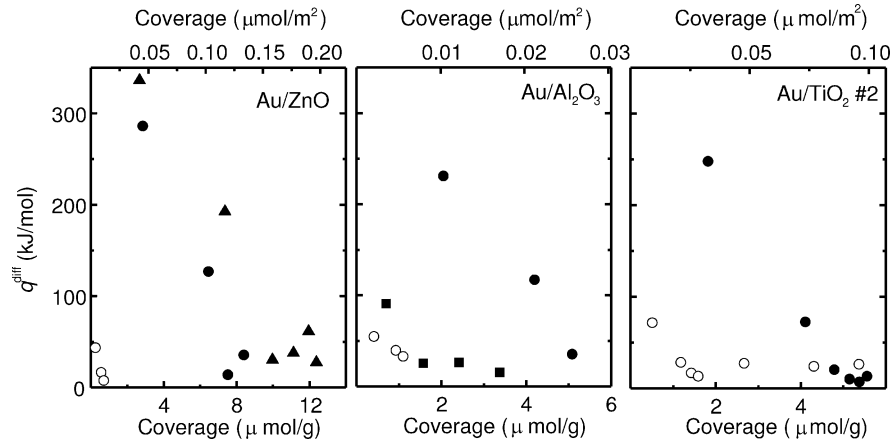

Figure 4. Differential heat of adsorption of CO on gold catalysts as a function of coverage in repeated adsorption measurements. (●) First isotherm after the pretreatment at 523 K in flowing 10% O_2 in Ar. (○) Second isotherm after CO adsorption and evacuation at 303 K. (▲) After oxidation in 100 kPa O_2 at 418 K within the calorimeter and evacuation. (■) After the O_2 isotherm (adsorption at $p < 1$ kPa) at 303 K and evacuation.

3.2. O_2 Uptake. The adsorption of O_2 on the gold catalysts was found to be much slower than that of CO. Figure 5 shows the adsorption kinetics of O_2 on Au/ZnO and Au/Al_2O_3. The coverage versus time profiles were measured after the first dose of each measurement series. Adsorption did not reach equilibrium under the experimental conditions of $p_{O_2} < 1$ kPa and $T = 303$ K. It is obviously a strongly activated process, and it was therefore not possible to reach equilibrium within the duration of the experiment. The difference in the uptake profiles between the first and second series of adsorption measurements on the Au/ZnO sample indicates that the adsorption of O_2 is also not reversible. Because adsorption equilibrium was not reached, q^{diff} of O_2 adsorption is only reliably determined at low coverages after the first dose in each experiment after CO adsorption and evacuation. The q^{diff} of O_2 adsorption on the Au/ZnO sample is derived to be 59 kJ/mol, and that value for other samples is below the detection limit.

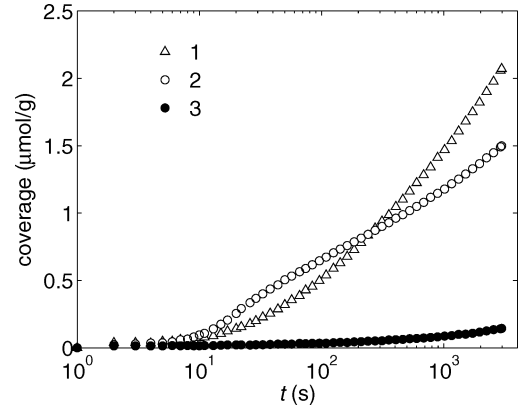

Figure 5. Adsorption kinetics of O_2 on Au catalysts. Au/Al_2O_3 first (1, △) O_2 adsorption after CO adsorption and evacuation. Au/ZnO first (2, ○) and second (3, ●) O_2 adsorption after CO adsorption and evacuation.

4. Discussion

4.1. Overlapping Reactions. The irreversible adsorption of CO and O_2 on the Au catalysts indicates that the exposed surfaces are very reactive. Multiple reactions can occur during adsorption, including adsorption of CO on the Au particles and on the support

$$CO + Au \rightarrow Au{-}CO \quad (5)$$

$$CO + M{-}O \rightarrow O{-}M{-}C{\equiv}O \quad (6)$$

For the reducible n-type semiconducting oxides ZnO and TiO_2, the reaction of CO with lattice oxygen or adsorbed oxygen can occur,

$$CO + M{-}O \rightarrow CO_2 + M{-}\square \quad (7)$$

followed by readsorption of CO_2,

$$CO_2 + M{-}O \rightarrow MCO_3 \quad (8)$$

and dissociative adsorption of oxygen.

$$O_2 + 2(M{-}\square) \rightarrow 2(M{-}O) \quad (9)$$

Reactions 7 and 9 form a Mars-van Krevelen redox cycle, involving oxygen vacancies denoted as □. By comparing the adsorption kinetics shown in Figures 3 and 5, we conclude that the adsorption of O_2 on the catalyst surface is a rather slow step. During the CO adsorption experiment, we found that the oxidation of CO and the formation of carbonates are irreversible. The difference between the uptake during the first and repeated series of adsorption measurements on an oxygen-pretreated sample summarized in Table 2 represents the amount of CO involved in reaction 7. The Au/ZnO sample (Figure 1, left) has the largest amount of lattice oxygen (7.6 μmol/g) that can be used for the oxidation of CO. As oxygen vacancies are assumed to be the active sites for CO hydrogenation over ZnO,[27] the role of these sites in Au/ZnO catalysts with varied Au loading was recently investigated applying steady state CO hydrogenation, followed by N_2O frontal chromatography.[56] Subsequent to exposure to the strongly reducing methanol synthesis conditions, the amount of consumed N_2O was found to increase in good correlation with the number of Au perimeter atoms present in the Au/ZnO catalysts, suggesting an enhanced formation of oxygen vacancies at the Au/ZnO interface. For the 1 wt % Au/ZnO catalyst, an amount of 8 μmol/g of consumed N_2O was derived, which is in excellent agreement with the amount of consumed CO of 7.6 μmol/g (Table 2).

On the basis of the measured reaction enthalpies

$$CO + 2{-}Zn{-}O{-} \rightarrow {-}Zn{-}O_2C{-}O{-} + {-}Zn{-}\square{-} \qquad \Delta H = -336\ \text{kJ/mol}$$

$$CO_2 + {-}Zn{-}O{-} \rightarrow {-}Zn{-}O_2C{-}O{-} \qquad \Delta H = -110\ \text{kJ/mol}$$

(from ref 61) and

$$CO + \frac{1}{2}O_2 \rightarrow CO_2 \qquad \Delta H = -283\ \text{kJ/mol}$$

(from ref 62) we obtain

$$-Zn{-}\square{-} + \frac{1}{2}O_2 \rightarrow {-}Zn{-}O{-} \qquad \Delta H = -57\ \text{kJ/mol}$$

This value is quite close to the result of O_2 adsorption on the Au/ZnO sample reduced by CO, demonstrating the reliability of the measurements of q^{diff}.

The areal amounts of consumed CO, summarized in Table 2, were derived by dividing by the specific surface areas (Table 1). Au/ZnO was found to be much more reducible than Au/TiO_2, and Au/Al_2O_3 had by far the lowest reducibility. For the latter sample, OH groups may be involved, which can react with CO to form a formate species. This reaction is also strongly exothermic. In general, the amounts of consumed CO per surface area are rather low, indicating that just a minor fraction of the exposed oxygen species can react with CO. Furthermore, the oxide surfaces, typically with 5−10 μmol/m^2 adsorption sites (Table 3), can easily accommodate the minor amount of formed CO_2 as carbonates, which are irreversibly bound at room temperature (eq 8).[63]

Diffusion of carbonate species created by the oxidation of CO is also a likely process during CO adsorption. The EPR spectroscopy study by Okumura et al.[64] showed that during CO oxidation over Au/TiO_2, active Ti centers are covered by carbonate species, which are not removed by CO or O_2. Thus, the inhibiting effect depends on the coverage of carbonates near the Au/support interface, and further depends on the diffusion rate of carbonates on the support surface, as indicated by Figure 3. The inhibiting effect does not seem to be present on the Au/ZnO sample. This may be related to the strong heterogeneity of the different exposed ZnO surfaces. The nonpolar ZnO($10\bar{1}0$) surface, which is composed of Zn−O dimers, is most favorable for the formation of stable adsorbed carbonates, but not for the formation of oxygen vacancies, which are only present on the polar ZnO($000\bar{1}$) surface.[65]

4.2. Thermodynamics of CO Adsorption. When adsorbing CO on Au catalysts, a group of overlapping reactions occurs. Yet, in the repeated adsorption, only the adsorption of CO on the Au particles and on the support are the dominating processes. The isotherms and heats of adsorption reflect these two overlapping processes and can be separated after careful analysis. Here, we apply a model, assuming uniform distributions of adsorption sites (subscript s) with different adsorption energies. The uptake of CO on the Au particles and on the support at equilibrium is a function of p, the adsorption energies of the most active sites $\varepsilon_{\max}$ and least active sites $\varepsilon_{\min}$ and the standard adsorption entropy Δs^0.[66]

$$\frac{n_s}{n_{m,s}} = \frac{RT}{\varepsilon_{\max,s} - \varepsilon_{\min,s}} \ln \frac{1 + \exp(\varepsilon_{\max,s}/RT + \Delta s_s{}^0/R)p/p^0}{1 + \exp(\varepsilon_{\min,s}/RT + \Delta s_s{}^0/R)p/p^0} \quad (10)$$

The subscripts Au and MO are for the gold and oxidic support, respectively. The uptake on the whole catalyst is the sum of that on Au and the support

$$n = n_{Au} + n_{MO} \quad (11)$$

The differential heat of adsorption on the Au sites or support sites is a function of the energy distribution and coverage[66]

$$q_s^{\text{diff}} = \varepsilon_{\max,s} - \frac{\left[\exp\left(\frac{\varepsilon_{\delta,s}}{RT}\right) - 1\right]\Theta - \left[\exp\left(\frac{\varepsilon_{\delta,s}\Theta_s}{RT}\right) - 1\right]}{\left[\exp\left(\frac{\varepsilon_{\delta,s}\Theta_s}{RT}\right) - 1\right]\left\{\exp\left[\frac{\varepsilon_{\delta,s}(1-\Theta_s)}{RT}\right] - 1\right\}}\varepsilon_{\delta,s} \quad (12)$$

where $\varepsilon_\delta = \varepsilon_{\max} - \varepsilon_{\min}$ is the scale parameter of the uniform distribution, and $\Theta = n/n_m$ is the fractional coverage. The differential heat of adsorption on the whole catalyst for each dose of the calorimetric measurement is averaged from that on Au and the support

$$q^{\text{diff}} = (\Delta n_{Au} q_{Au}^{\text{diff}} + \Delta n_{MO} q_{MO}^{\text{diff}})/(\Delta n_{Au} + \Delta n_{MO}) \quad (13)$$

The parameters for the best fit of the above models to the experimental data are summarized in Table 3. The density of

exposed Au atoms on the catalyst surfaces ($n_{m,Au}$) is derived from the Au content and particle size and that of the metal cations ($n_{m,MO}$) from the crystal structure of the supports. The standard adsorption entropies of CO on the different supports are taken from the measurements reported in the literature.[67,68,69] Only the standard adsorption entropy of CO on Au and the adsorption energy distribution is needed to be fitted, thus the fitting is considered rigorous.

Figure 6 shows the evaluation of the isotherms of the second series of CO adsorption experiments on each catalyst. Each isotherm is composed of CO adsorption on the Au particles and the support. The former tends to saturate at the experimental pressure, while the latter shows a linear increase of coverage with p, which is typical for adsorption at a very low fractional coverage. The ratio between the adsorbed amount on Au and on the support decreases with increasing CO pressure. When the pressure is high enough, the amount on Au is negligible, which may explain the results obtained by Iizuka et al.,[33] who concluded that CO adsorption on Au/TiO_2 appeared to be of the Langmuirian type.

For comparison, the thermodynamic parameters of CO adsorption on the Au(110) single crystal surface and on Au catalysts are also derived from the isobars reported in the literature.[40,43,44] Equation 10 is applied to evaluate the isobars; the change of Δs^0 is considered in the following way

$$\Delta s^0(T) = s_{vib}^{\sigma,0} - s_{rot}^{CO,0}(T) - s_{trans}^{CO,0}(T) \qquad (14)$$

where $s_{trans,CO}^0$ and $s_{rot,CO}^0$ are the standard entropy of CO in the gas phase contributed by translation and rotation, respectively, and $\Delta s_{vib}^{\sigma,0}$ is the vibrational entropy of the adsorbates, which does not vary with temperature. The values of $s_{CO}^0(T)$ and $s_{trans}^{CO,0}(T)$ are known from the statistical thermodynamics.[70] Therefore, by fitting eq 10 to the isobars, the adsorption entropy and the distribution of the adsorption energy can be derived.

The results of the analysis of the isobars of CO adsorption on Au catalysts reported in literature are shown in Figure 7 and Table 4.[40,43,44] Figure 7 shows that the isobars can be well-described by the model. The parameters for CO adsorption on Au/TiO_2 are similar to Table 3, indicating that the model is highly reliable.

The adsorption energies and entropies summarized in Tables 3 and 4 show that the chemical nature of the support has a considerable effect on the interaction between CO and the Au particles. CO interacts most strongly with Au particles supported on TiO_2 as indicated by the highest ε_{max} and entropy loss. The entropy of adsorption reflects the adsorbate−adsorbent interactions as well as the mobility of the adsorbates. The large entropy loss of CO on Au/TiO_2 indicates that the vibrational entropy contributed by adsorbed CO is rather small, which is attributed to back-bonding from the Au site to the antibonding $2\pi^*$ orbital of adsorbed CO. The adsorption energy of CO on Au/ZnO is close to that of CO on Au/Al_2O_3, but the entropy loss of the former is smaller. Thus, the adsorption energies and entropy losses suggest the following sequence concerning the interaction between the Au particles and different supports: Au/TiO_2 > Au/

TABLE 3: Thermodynamic Parameters for the Theoretical Evaluation of CO Adsorption on Gold Catalysts

	adsorption on support				adsorption on Au			
sample	$n_{m,MO}$	Δs^0	$\varepsilon_{max}{}^a$	$\varepsilon_\delta{}^a$	$n_{m,Au}{}^b$	Δs^a	$\varepsilon_{max}{}^a$	$\varepsilon_\delta{}^a$
Au/ZnO	9.8[c]	−102[67]	37	26	0.049	−87	60	50
Au/Al_2O_3	9.4[d]	-122 ± 18[e]	41	90	0.054	−120	59	50
Au/TiO_2 #1	4.75[f]	−110[68]	41	7	0.060	−150	98	30
Au/TiO_2 #2	4.75[f]	−110[68]	41	18	0.090	−150	77	48

[a] Fitted result. [b] Calculated from the gold content and gold particle size. Units are n [μmol/m^2_{cat}], S [J mol^{-1} K^{-1}], and ε [kJ/mol]. [c] Density of Zn^{2+} on ZnO($10\bar{1}0$). [d] Density of Al^{3+} on the surfaces of γ-alumina. [e] Derived from ref 69. [f] Density of Ti^{4+} on TiO_2 (110).

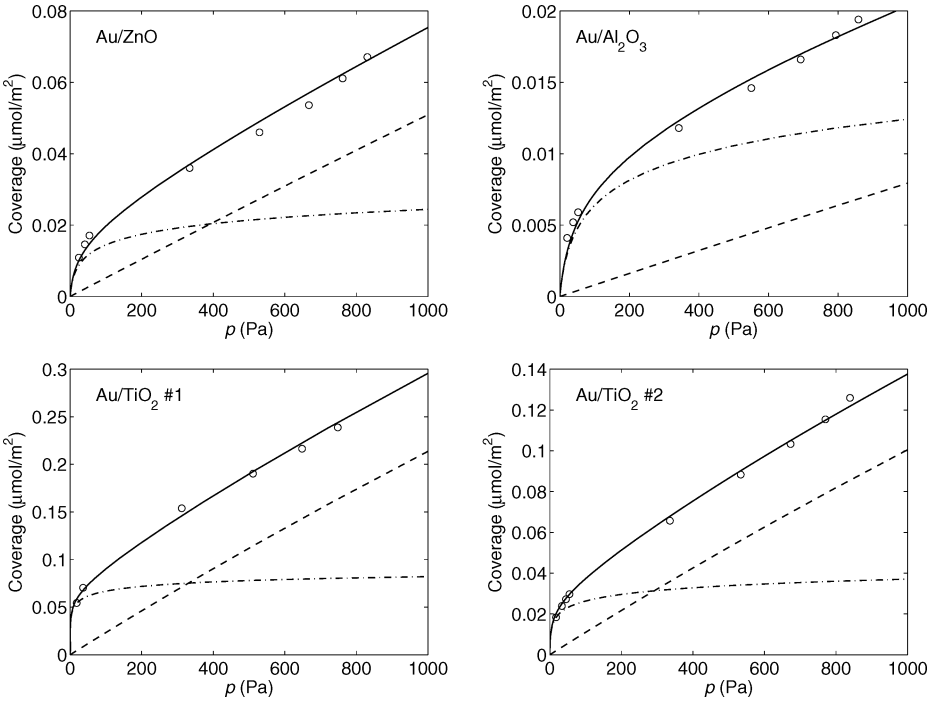

Figure 6. Fitting the isotherms of the second series of CO adsorption experiments (solid lines) after evacuation of the initially oxidized samples to two overlapping adsorption processes on Au sites (dashed−dotted lines) and on the support (dashed lines).

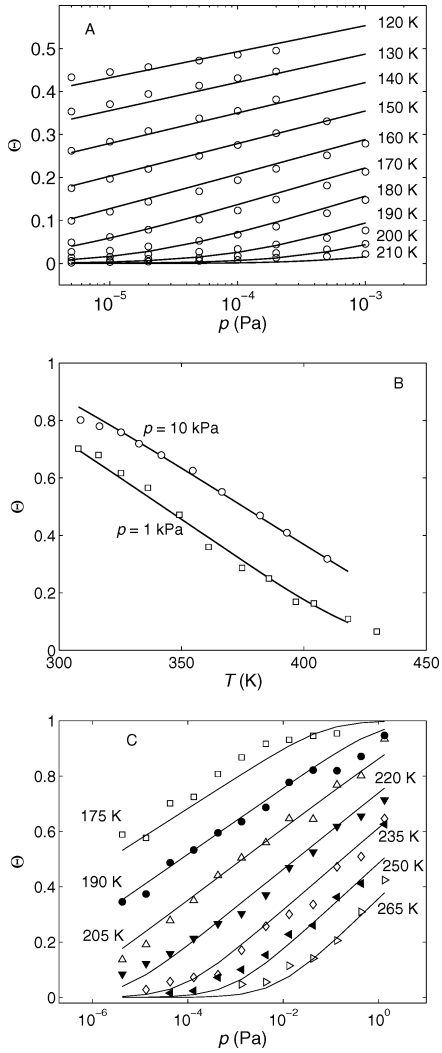

Figure 7. Fittings of the uniform model of CO adsorption energy to published experimental data on different Au samples. (A) Au(110),[40] (B) Au sites on Au/TiO_2,[44] and (C) Au sites on Au/TiO_2.[43]

TABLE 4: Thermodynamics of CO Adsorption on Au Derived from Isobars Reported in the Literature[40,43,44]

sample	ε_{max} (kJ/mol)	ε_δ (kJ/mol)	Δs^0 (298 K) (J mol^{-1} K^{-1})
Au(110)[a]	46	37	−84
Au/TiO_2[b]	69	19	−146
Au/TiO_2[c]	83	38	−146

[a] Source of isobars: Source of isobar is ref 40. [b] Source of isobar is ref 44. [c] Source of isobar is ref 43.

Al_2O_3 > Au/ZnO. It is interesting to note that the same sequence was found for the catalytic CO oxidation activity.[57]

Further studies using FTIR spectroscopy and isotopically labeled reactants in a ultrahigh vacuum (UHV) system equipped with a high-pressure cell are in progress to elucidate the role of residual OH groups and to identify the CO oxidation products following the pioneering FTIR studies by Boccuzzi and co-workers.[71,72]

5. Conclusions

Several overlapping processes were detected during the interaction of CO as weakly adsorbing probe molecules with supported Au catalysts, including adsorption of CO on the Au particles and support, oxidation of CO by lattice oxygen, and diffusion of carbonates and oxygen vacancies. On preoxidized Au samples, the initial heat of these processes was over 200 kJ/mol. Correspondingly, because of the redox processes, CO adsorption was not reversible. The adsorption rate of O_2 on the Au catalysts was much slower than that of CO, which may be retarded by the diffusion of oxygen vacancies. The energy distributions and standard entropies of adsorption of CO on the Au sites were derived. The interaction between CO and Au on TiO_2 was found to be much stronger than that on ZnO, which is ascribed to back-bonding from the Au sites to CO. The Au/ZnO sample had significantly different properties compared with those of the Au/Al_2O_3 and Au/TiO_2 samples, including a larger amount of removable lattice oxygen, higher heats of adsorption of CO on the oxidized samples in the first series of adsorption experiments and of O_2 on the CO-reduced samples, less inhibition by carbonates created by oxidation, and a weaker interaction between CO and Au in the second series of adsorption experiments after evacuation.

Acknowledgment. The authors thank Bernd Meyer, Yuemin Wang, and Christof Wöll for fruitful discussions and the Deutsche Forschungsgemeinschaft (DFG) for financial support within the Collaborative Research Center (SFB 558) "Metal-Substrate Interactions in Heterogeneous Catalysis".

References and Notes

(1) Davies, P. Snowden, F. F. Bridger, G. W. Hughes, D. O. Young, P. W. GB 1,010,817 ICI.
(2) Natta, G. *Synthesis of Methanol Catalysis*, Vol. 3; Reinhold Publishing Corporation: New York, 1955; p 349.
(3) Sakurai, H.; Haruta, M. *Appl. Catal., A* **1995**, *127*, 93.
(4) Sakurai, H.; Haruta, M. *Catal. Today* **1996**, *29*, 361.
(5) Nomura, N.; Tagawa, T.; Goto, S. *React. Kinet. Catal. Lett.* **1998**, *63*, 9.
(6) Zhao, Y.; Mpela, A.; Enache, D. I.; Taylor, S. H.; Hildebrandt, D.; Glasser, D.; Hutchings, G. J.; Atkins, M. P.; Scurell, M. S. *Stud. Surf. Sci. Catal.* **2007**, *163*, 141.
(7) Mpela, A.; Hildebrandt, D.; Glasser, D.; Scurrell, M. S.; Hutchings, G. J. *Gold Bull.* **2007**, *40*, 219.
(8) Clausen, B. S.; Schiøtz, J.; Grabaek, L.; Ovesen, C. V.; Jacobson, K. W.; Nørskov, J. K.; Topsøe, H. *Top. Catal.* **1994**, *1*, 367.
(9) Grunwaldt, J.-D.; Molenbroek, A. M.; Topsøe, N.-Y.; Topsøe, H.; Clausen, B. S. *J. Catal.* **2000**, *194*, 452.
(10) Jung, K.-D.; Joo, O.-S.; Han, S.-H. *Catal. Lett.* **2000**, *68*, 49.
(11) Spencer, M. S. *Top. Catal.* **1999**, *8*, 259.
(12) Wilmer, H.; Hinrichsen, O. *Catal. Lett.* **2002**, *82*, 117.
(13) Greeley, J.; Gokhale, A. A.; Kreuser, J.; Dumesic, J. A.; Topsøe, H.; Topsøe, N.-Y.; Mavrikakis, M. *J. Catal.* **2003**, *213*, 63.
(14) Wagner, J. B.; Hansen, P. L.; Molenbroek, A. M.; Topsøe, H.; Clausen, B. S.; Helveg, S. *J. Phys. Chem. B* **2003**, *107*, 7753.
(15) Nakamura, J.; Choi, Y.; Fujitani, T. *Top.Catal.* **2003**, *22*, 277.
(16) Naumann d'Alnoncourt, R.; Kurtz, M.; Wilmer, H.; Löffler, E.; Hagen, V.; Shen, J.; Muhler, M. *J. Catal.* **2003**, *220*, 249.
(17) Naumann d'Alnoncourt, R.; Xia, X.; Strunk, J.; Löffler, E.; Hinrichsen, O.; Muhler, M. *Phys. Chem. Chem. Phys.* **2006**, *8*, 1525.
(18) Kuznetsov, V. D.; Shub, F. S.; Temkin, M. I. *Kinetika i Kataliz* **1982**, *23*, 932.
(19) Kagan, Yu. B.; Rozovskii, A.Ya.; Liberov, L. G.; Slivinskii, E. V.; Lin, G. I.; Loktev, S. M.; Bashkirov, A. N. *Dokl. Akad. Nauk. SSSR* **1975**, *224*, 1081.
(20) Chinchen, G. C.; Denny, P. J.; Parker, D. G.; Spencer, M. S.; Whan, D. A. *Appl. Catal.* **1987**, *30*, 333.
(21) Liu, G.; Willcox, D.; Garland, M.; Kung, H. H. *J. Catal.* **1985**, *96*, 251.
(22) Muhler, M.; Törnqvist, E.; Nielsen, L. P.; Clausen, B. S.; Topsøe, H. *Catal. Lett.* **1994**, *25*, 1.
(23) Chinchen, G. C.; Denny, P. J.; Jennings, J. R.; Spencer, M. S.; Waugh, K. C. *Appl. Catal.* **1988**, *36*, 1.
(24) Bridger, G. W. Spencer, M. S. Methanol Synthesis, In *Catalyst Handbook*, 2nd ed.; M.V. Twigg, Manson Publishing: London, 1996; p 441.
(25) Rhodes, C.; Hutchings, G. J.; Ward, A. M. *Catal. Today* **1995**, *23*, 43.
(26) Amadeo, N. E.; Laborde, M. A. *Trends Chem. Eng.* **1996**, *3*, 159.
(27) Kurtz, M.; Strunk, J.; Hinrichsen, O.; Muhler, M.; Fink, K.; Meyer, B.; Wöll, Ch. *Angew. Chem., Int. Ed.* **2005**, *44*, 2790.

(28) French, S. A.; Sokol, A. A.; Bromley, S. T.; Catlow, C. R. A.; Rogers, S. C.; King, F.; Sherwood, P. *Angew. Chem., Int. Ed.* **2001**, *40*, 4437.
(29) French, S. A.; Sokol, A. A.; Bromley, S. T.; Catlow, C. R. A. *Top. Catal.* **2003**, *24*, 161.
(30) Polarz, S.; Strunk, J.; Ischenko, V.; van den Berg, M. W. E.; Hinrichsen, O.; Muhler, M. *Angew. Chem., Int. Ed.* **2006**, *45*, 2965.
(31) Shastri, A. G.; Datye, A. K.; Schwank, J. *J. Catal.* **1984**, *87*, 265.
(32) Lin, S. D.; Bollinger, M.; Vannice, M. A. *Catal. Lett.* **1993**, *17*, 245.
(33) Iizuka, Y.; Fujiki, H.; Yamauchi, N.; Chijiiwa, T.; Arai, S.; Tsubota, S.; Haruta, M. *Catal. Today* **1997**, *36*, 115.
(34) Cant, N. W.; Ossipoff, N. J. *Catal. Today* **1997**, *36*, 125.
(35) Boccuzzi, F.; Chiorino, A.; Tsubota, S.; Haruta, M. *Sens. Actuators* **1995**, *B25*, 540.
(36) Bondzie, V. A.; Parker, S. C.; Campbell, C. T. *Catal. Lett.* **1999**, *63*, 143.
(37) Schubert, M. M.; Hackenberg, S.; van Veen, A. C.; Muhler, M.; Plzak, V.; Behm, R. J. *J. Catal.* **2001**, *197*, 113.
(38) Elliott, G. S. Miller, D. R. *Proceedings of the 14th International Symposium on Rarefied Gas Dynamics*; University of Tokyo Press: Tokyo, 1984; p 349.
(39) Ruggiero, C.; Hollins, P. *J. Chem. Soc., Faraday Trans.* **1996**, *92*, 4829.
(40) Gottfried, J. M.; Schmidt, K. J.; Schroeder, S. L. M.; Christmann, K. *Surf. Sci.* **2003**, *536*, 206.
(41) McElhiney, G.; Pritchard, J. *Surf. Sci.* **1976**, *60*, 397.
(42) Meier, D. C.; Bukhtiyarov, V.; Goodman, D. W. *J. Phys. Chem. B* **2003**, *107*, 12668.
(43) Meier, D. C.; Goodman, D. W. *J. Am. Chem. Soc.* **2004**, *126*, 1892.
(44) Derrouiche, S.; Gravejat, P.; Bianchi, D. *J. Am. Chem. Soc.* **2004**, *126*, 13010.
(45) Winkler, C.; Carew, A. J.; Haq, S.; Raval, R. *Langmuir* **2003**, *19*, 717.
(46) Diemant, T.; Hartmann, H.; Bansmann, J.; Behm, R. J. *J. Catal.* **2007**, *252*, 171.
(47) Shaikhutdinov, Sh. K.; Meyer, R.; Naschitzki, M.; Bäumer, M.; Freund, H.-J. *Catal. Lett.* **2003**, *86*, 211.
(48) Manzoli, M.; Boccuzzi, F.; Chiorino, A.; Vindigni, F.; Deng, W.; Flytzani-Stephanopoulos, M. *J. Catal.* **2007**, *245*, 308.
(49) Hadjiivanov, K. I.; Vayssilov, G. N. *Adv. Catal.* **2002**, *47*, 307.
(50) Bond, G. C.; Louis, C.; Thompson, D. T. *Catalysis by Gold*; Hutchings, G. J., Ed.; Catalytic Science Series; Imperial College Press: London, 2006; Vol. 6.
(51) Chen, Y.; Crawford, P.; Hu, P. *Catal. Lett.* **2007**, *119*, 21.
(52) Tripathi, A. K.; Kamble, V. S.; Gupta, N. M. *J. Catal.* **1999**, *187*, 332.
(53) Gupta, N. M.; Tripathi, A. K. *J. Catal.* **1999**, *187*, 343.
(54) Sault, A. G.; Madix, R. J.; Campbell, C. T. *Surf. Sci.* **1986**, *169*, 347.
(55) Haruta, M.; Tsubota, S.; Kobayashi, T.; Kageyama, H.; Genet, M. J.; Delmon, B. *J. Catal.* **1993**, *144*, 175.
(56) Strunk, J.; Kähler, K.; Xia, X.; Comotti, M.; Schüth, F.; Reinecke, T.; Muhler, M. *Appl. Catal., A* **2009**, *359*, 121.
(57) Comotti, M.; Li, W.-C.; Spliethoff, B.; Schüth, F. *J. Am. Chem. Soc.* **2006**, *128*, 917.
(58) Tsubota, s.; Yamaguchi, A.; Daté, A.; Haruta, M. *Gold Bull.* **2003**, *36*, 24.
(59) Xia, X.; Naumann d'Alnoncourt, R.; Strunk, J.; Litvinov, S.; Muhler, M. *J. Phys. Chem. B* **2006**, *110*, 8409.
(60) Xia, X. *Experimental and Theoretical Aspects of Adsorption Microcalorimetry Applied to Characterize Heterogeneous Catalysts*. Ph.D. Thesis, Ruhr-University Bochum, Germany, 2006.
(61) Xia, X.; Strunk, J.; Busser, W.; Naumann d'Alnoncourt, R.; Muhler, M. *J. Phys. Chem. C* **2008**, *112*, 10938.
(62) Lide, D. R. *Handbook of Chemistry and Physics*; CRC Press: London, 2005.
(63) Henrich, V. H. Cox, P. A. *The Surface Science of Metal Oxides;* Cambridge University Press: Cambridge, U.K., 1994.
(64) Okumura, M.; Coronado, J. M.; Soria, J.; Haruta, M.; Conesa, J. C. *J. Catal.* **2001**, *203*, 168.
(65) Wöll, Ch. *Prog. Surf. Sci.* **2007**, *82*, 55.
(66) Xia, X.; Litvinov, S.; Muhler, M. *Langmuir* **2006**, *22*, 8063.
(67) Xia, X.; Strunk, J.; Naumann d'Alnoncourt, R.; Busser, W.; Khodeir, L.; Muhler, M. *J. Phys. Chem. C* **2008**, *112*, 10931.
(68) Xia, X.; Busser, W.; Strunk, J.; Muhler, M. *Langmuir* **2007**, *23*, 11063.
(69) Cabrejas Manchado, M.; Guil, J. M.; Pérez, A.; Ruiz Paniego, A.; Trejo Menayo, J. M. *Langmuir* **1994**, *10*, 685.
(70) McQuarrie, D. A. *Statistical Thermodynamics*; University Science Books: Herndon, VA, 1985; Vol. 81.
(71) Boccuzzi, F.; Chiorino, A.; Tsubota, S.; Haruta, M. *J. Phys. Chem.* **1996**, *100*, 3625.
(72) Boccuzzi, F.; Chiorino, A. *J. Phys. Chem. B* **2000**, *104*, 5414.

JP809804V